Original article

Sulfanilamide in solution and liposome vesicles; *in vitro* release and UV-stability studies

Sanja Petrović [a,*], Ana Tačić [a], Saša Savić [a], Vesna Nikolić [a], Ljubiša Nikolić [a], Sanela Savić [b,c]

[a] *University of Nis – Faculty of Technology, Department of Organic and Technological Sciences, Bulevar Oslobodjenja 124, 16000 Leskovac, Serbia*
[b] *University of Belgrade – Faculty of Pharmacy, Department of Pharmaceutical Technology and Cosmetology, Vojvode Stepe 450, 11221 Belgrade, Serbia*
[c] *DCP Hemigal, Tekstilna 97, 1600 Leskovac, Serbia*

A R T I C L E I N F O

A B S T R A C T

The main goal of this study was to develop a liposome formulation with sulfanilamide and to investigate the liposomes impact on its release and stability to the UV-A/UV-B and UV-C irradiation. Liposome dispersions with incorporated sulfanilamide were prepared by thin-film hydration method and liposomes role to the sulfanilamide release was investigated by using a dialysis method. Comparatively, sulfanilamide in phosphate buffer solution was subject to release study as well to the UV irradiation providing for the possibilities of kinetics analysis. *In vitro* drug release study demonstrated that 20% of sulfanilamide was released from liposomes within 1 h that is approximately twice as slower as in the case of dissolved sulfanilamide in phosphate buffer solution. The kinetic release process can be described by Korsmeyer–Peppas model and according to the value of diffusion release exponent it can be concluded that drug release mechanism is based on the phenomenon of diffusion. The sulfanilamide degradation in phosphate buffer solution and liposomes is related to the formation of UV-induced degradation products that are identified by UHPLC/MS analysis as: sulfanilic acid, aniline and benzidine. The UV-induced sulfanilamide degradation in the phosphate buffer solution and liposome vesicles fits the first- order kinetic model. The degradation rate constants are dependent on the involved UV photons energy input as well as sulfanilamide microenvironment. Liposome microenvironment provides better irradiation sulfanilamide stability. The obtained results suggest that liposomes might be promising carriers for delayed sulfanilamide delivery and may serve as a basis for further research.

1. Introduction

Sulfanilamide, 4-aminobenzenesulfonamide (SA) belongs to a group of sulfonamides, the synthetic antimicrobial drug agents, commonly used in treatments against Gram-positive and Gram-negative bacteria as well as in the treatments of fungi and protozoa infections (Henry, 1943; Gray et al., 1995; Sukul and Spiteller, 2006; Varagić and Milošević, 2009). Because of heteroatoms, aromatic ring and other functional chromophore groups in the structure that are sensitive to solar radiation, sulfonamides are

considered unstable. Photocatalytic degradation of sulfonamides may occur due to absorption of solar radiation (direct photocatalysis), or by reactive free radicals action such as singlet oxygen, hydroxyl radicals and other reactive species (indirect photocatalysis) (Lam and Mabury, 2005). Photodegradation efficiency in an aqueous medium depends on the intensity and frequency of applied radiation treatment, medium pH (Trovó et al., 2009; Baran et al., 2006) as well as of a photosensitizer, such as humic acid and nitrates, which can be present in the solution. A pH affects the degradation reaction rate, but does not affects the type of the degradation products in the reaction mentioned above (Boreen et al., 2004). Zessel et al. (2014) examined the sulfonamides stability to degradation under the influence of UV-A irradiation, a combination of UV-A and UV-B irradiation and sunlight. The results showed that all investigated sulfonamides are subject to degradation under the action of UV irradiation. Photo degradation was most pronounced after exposure to combined UV-A/UV-B irradiation, then after the UV-A, and finally after exposure to sunlight irradiation. The sulfonamides have a different inclination towards

photo degradation depending on the chemical structure; thus, sulfathiazole and SA were almost completely decomposed after only 4 h of UV-A/UV-B irradiation. Of all investigated sulfonamides, sulfamethoxypyridazine, sulfachloropyridazine and SA had the greatest degree of degradation (31–65%) when exposed to UV-A irradiation. Photocatalytic degradation of various sulfonamides in the aqueous solution resulted in the formation of different degradation products, including the most commonly present sulfanilic acid, aniline, hydroquinone, carboxylic and dicarboxylic acids. The most possible degradation routes include severing S—N bonds and a loss of SO_2 molecule (Periša et al., 2013). In addition, hydroxylation of benzene ring (Trovó et al., 2009) and R residue that are bonded to the nitrogen of the sulfonamide groups are also possible degradation reactions (Lam and Mabury, 2005).

In addition to these data, there is generally a lack of information's about SA stability and possible degradation products. Because of that, there is a great need for new analytical methods capable to determine SA degradation products that are produced after *in vitro* or *in vivo* oxidation caused by free radicals acting. Also, there is a great need to determine the SA stability in pharmaceutical as well as cosmetics formulations because of wide use of this active compound. On the other hand, due to poor solubility of SA in the aqueous medium (Delgado et al., 2011), the SA use is limited. In order to improve the SA solubility and photostability, SA was incorporated in liposomes.

In this work we have investigated SA stability under influence of UV (UV-A, UV-B and UV-C) irradiation in phosphate buffer solution (PBS) and in liposomes the commonly used vesicular carriers for targeted therapies. After incorporation in liposomes, SA release from the liposomes was also investigated. In order to investigate the liposome size influence on distribution and activity of incorporated SA, three types of liposomes: small unilamellar vesicles (SUV), large unilamellar liposomes (LUV) and multi lamellar vesicles (MLV) were obtained. SA was irradiated in PBS and in liposomes but this time UHPLC techniques in combination with absorption spectroscopy were employed to analyze the formation of SA degradation products induced by continuous UV irradiation to provide the data for a kinetic analysis. The results obtained in this work may serve for further investigations of SA activity in active formulations. Also, applied optimized UHPLC-MS-MS method for identifying degradation products generated under UV irradiation can be regarded as selective, rapid and sensitive and may serve to further studies.

2. Materials and method

2.1. Materials

1.2-Diacyl-*sn*-glycero-3-phosphocholine (PC, critical temperature Tc = 15 °C) was purchased from Sigma Aldrich (Germany) and used without further purification. According to the declaration statement the PC mixture has the following fatty acid composition: 33% palmitic acid, 13% stearic acid, 31% oleic and 15% linoleic acid (other fatty acid were present in a negligible amount). The phosphate buffer solution (Na_2HPO_4-KH_2PO_4, pH 7.4), was prepared using analytical grade reagents (Centrohem, Serbia) and purified water from a Millipore Milli-Q system (conductivity $\leq 0.1\ \mu S \cdot cm^{-1}$). All other materials and solvents were of analytical grade.

2.2. Sulfanilamide synthesis

Procedure of SA synthesis was carried out as previously described (Tačić et al., 2014). Chlorosulfonic acid together with acetanilide was heated for 1 h at 65 °C and then cooled. The separated crystals of 4-(acetylamino)benzenesulfonyl chloride were

dissolved in water after ammonia was added and left for 24 h. The filtered crystals in the round flask were then treated with sodium hydroxide and heated under reflux. The concentrated hydrochloric acid was carefully added into the mixture, and then neutralized. The obtained SA was recrystallized from the water in order to obtain the pure substance.

2.3. Liposomes preparation

MLV, LUV and SUV liposomes with incorporated SA were prepared according to the thin-film hydration method, as previously described (Milenkovic et al., 2013; Petrović et al., 2014) with slight modifications. The PC lipid was dissolved in chloroform at the molar concentration of 5×10^{-4} M. The SA dissolved in PBS was added to the lipid at the concentration of 1×10^{-5} M, considering the final buffer volume of liposome suspension. The obtained liposome dispersions after preparation procedure were MLVs. In order to obtain LUVs and SUVs, the liposome dispersion was vortexed (HI 190M, Hanna instruments, Italy) at a speed of 500 rpm, and then extruded (LiposoFast-Basic Extruder, Avestin, Inc. Canada) through poly-carbon filters of 400 and 100 nm pore size respectively. UV–Vis absorption spectroscopy was used to rapidly estimate the dimension and lamellarity of liposomes with incorporated SA. All the operations have been performed above the critical temperature (Tc) of lipid in order to avoid defects. After preparation, all dispersions were stored at 4 °C and after 24 h their characterization was performed. The spectral data have been processed by using the software Origin 8.0.

2.4. In vitro SA release from liposomal dispersions

SA release from MLV liposomes was studied using a dialysis method. Before use, the dialysis bags (dialysis tubing cellulose membrane, Sigma Aldrich, *Mr.* cut-off 12,000 (Germany)) were soaked in PBS at a room temperature of 23 °C for 24 h to remove the preservative, followed by rinsing thoroughly in distilled water. Liposomal dispersion, 5 mL, was placed in dialysis bag of 11 cm initial length and 43 mm flat width. The bag was closed at both ends with plastic clips and tested for leakage. The final length of the bag after tying was 3 ± 0.2 cm. The dialysis bag was attached horizontally, fully stretched to the magnet on magnetic stirrer, which was then immersed in the 150 mL glass containing 50 mL of PBS pH 7.4. The bag was fully immersed under the surface. The temperature was set at 23 ± 0.2 °C and the rotation speed was set at 100 rpm to simulate *in vivo* conditions. Control bags were prepared and tested along with the liposomal dispersions. Aliquots of the release medium were withdrawn for analysis at different time intervals. Release runs were continued for 2 h. The absorbance of the collected samples was measured at SA max absorption at 258 nm. Control SA release was also run at the same conditions, from the SA-PBS pH 7.4 and identical SA concentration as in liposome dispersion. SA release kinetics in liposome and PBS was evaluated using different mathematical models (zero order, first order, Higuchi, Korsmeyer-Peppas, Baker-Lonsdale), using *DDSolver* package for *Microsoft Excel* application.

2.5. SA photostability study

The SA samples in PBS and in liposomes were exposed to the UV-A UV-B and UV-C irradiation. The samples were treated by UV-A irradiation in a period of 0–150 min, UV-B irradiation in a period of 0–3 min and UV-C irradiation in a period of 0–0.5 min in the cylindrical photochemical reactor "Rayonnet" with 10 symmetrically placed UV-A and UV-B and 8 UV-C lamps having an emission maximum at 350 nm (UV-A), 300 nm (UV-B) and 254 nm (UV-C), respectively. The quartz cells ($1 \times 1 \times 4.5$ cm)

placed on a circular rotating holder was used. The total measured energy flux (hitting the samples) was about $12.86\ W/m^2$ for UV-A, $15\ W/m^2$ for UV-B and $14.29\ W/m^2$ for UV-C irradiation respectively, at a distance of 10 cm from the lamps. The samples were filtered through the cellulose membrane of 0.45 μm (Econofilters, Agilent Technologies, Germany) and analyzed by the UV–Vis method as well as UHPLC/MS analysis to detected products of irradiation.

2.6. Spectral measurements

The optical absorption spectra were obtained on a double beam Varian Cary-100 spectrophotometer equipped with 1.0 cm quartz cells. All spectra were recorded from 190 to 800 nm with 1.0 bandwidth.

2.7. UHPLC-DAD-HESI-MS/MS analysis

UHPLC-DAD-HESI-MS/MS analysis was performed by using a Thermo Scientific liquid chromatography system (UHPLC) composed of a quaternary pump with a degasser, a thermostated column compartment, an autosampler, and a diode array detector connected to LCQ Fleet Ion Trap Mass Spectrometer (Thermo Fisher Scientific, San Jose, California, USA) equipped with heated electrospray ionisation (HESI). Xcalibur (version 2.2 SP1.48) and LCQ Fleet (version 2.7.0.1103 SP1) software were used for instrument control, data acquisition and data analysis. Separations were performed on a Hypersil gold C18 column (50×2.1 mm, 1.9 μm) obtained from Thermo Fisher Scientific.

The mobile phase consisted of (A) water + 0.1% formic acid and (B) acetonitrile. A linear gradient program at flow rate of 0.250 mL/min was used 0–2 min from 10 to 20% (B), 2–4.5 min from 20 to 90% (B), 4.5–4.8 min 90% (B), 4.8–4.9 min from 90 to 10% and 4.9–10.0 min 10% (B). The injection volume was 10 μL, and the column temperature was maintained at 25 °C. The separated compounds were detected at a wavelength of 208, 234, 260 and 583 nm, and each online spectrum was recorded within the range of 200–800 nm. The mass spectrometer was operated in positive mode. HESI-source parameters were as follows: source voltage 4.5 kV, capillary voltage 19 V, tube lens voltage 20 V, capillary temperature 275 °C, sheath and auxiliary gas flow (N_2) 50 and 8 (arbitrary units), respectively. MS spectra were acquired by full range acquisition covering 50–1000 m/z. For fragmentation study, a data dependent scan was performed by deploying the collision-induced dissociation (CID). The normalized collision energy of the CID cell was set at 25 eV. All compounds were identified according to the corresponding spectral characteristics: mass spectra, accurate mass and characteristic fragmentation.

3. Results and discussion

3.1. UV–Vis spectroscopy studies

UV–Vis absorption spectra of liposomes (SUV, LUV and MLV) with incorporated SA are presented in Fig. 1. The spectrum of the SA in PBS, at a concentration of 1×10^{-5} M is jointly presented in the Fig. 1. Based on previous studies (Silverstein et al., 2014; Khankhasaeva et al., 2015) it is known that the absorption spectrum of SA has one intense absorption band at about 260 nm. The central SA chromophore has a benzene ring with a maximum absorbance of about 255 nm, however, due to the presence of amino groups and free electron pairs derived from nitrogen, there is bathochromic shift of main absorption band of SA.

The liposomes scatter light and the absorption spectra are affected so that baseline is shifted from the x-axis in the case of
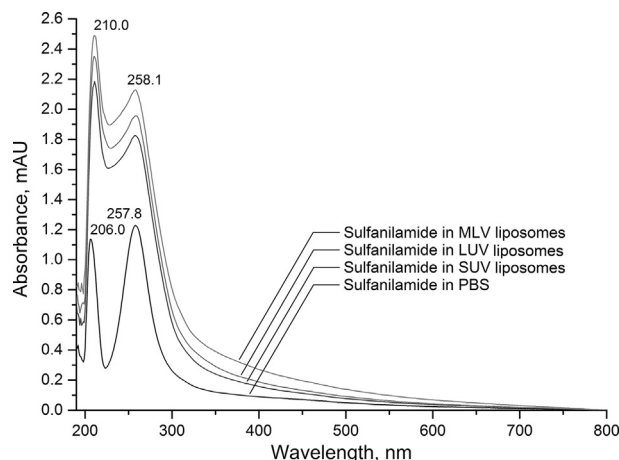

Fig. 1. UV–Vis spectra of SA incorporated in PC-SUV/LUV and MLV liposomes joined with the SA-PBS spectra. The SA concentration was 1×10^{-5} M. The final SA/lipid ratio was 1/50.

SA-SUV/LUV and MLV liposomes. The light scattering presented by MLV suspensions differs from that of the SUV and LUV vesicles (Wittung et al., 1994). The Rayleigh scattering applies for particles with radius (R) shorter than $\lambda/20$ (R < $\lambda/20$) and this "rule" provides a rapid estimation of the liposomes dimension (Patrascu et al., 2010). The spectra of SA in SUV/LUV/MLV and SA in PBS are similar as regarding the shape. Regarding to peak positions, the spectra of SA in liposomes is moved bathochromic (from 257.8 to 258.1), due to different SA micro environment. The possible way of SA incorporation in liposomes is in the liposome polar interior. It is likely to consider that the shift of the SA red maximum in liposomes is due to the polar environment in which the SA macrocycle is located – the water interface in the liposomes interior.

3.2. Release SA-liposomes studies

Unlike most pharmaceutical forms, for cosmetics preparations as well as liposome dispersions there is no standard or other regulatory prescribed method for in vitro release rate determination of the incorporated active compounds (Burgess et al., 2002; Brown et al., 2011; Shen and Burgess, 2012). Most commonly used methods for these kinds of researches are: sample-and-separate, continuous flow, in situ, and membrane barrier methods that include side-by-side diffusion cell and dialysis sac/bag method (Chidambaram and Burgess, 1999). Active substance release from vesicle carriers can be influenced by both the membrane composition of the carrier and the structure of incorporated active compound-drug. In this study, in vitro release rate of SA in liposomes was carried out using the techniques with dialysis bags (Chidambaram and Burgess, 1999). In the obtained test, SA liposome dispersion acts as a donor in the dialysis until PBS medium in the outer of the bag acts as acceptor phase. Percentage of SA release from the investigated liposome delivery dispersions as well as control PBS was calculated in predefined time intervals (Fig. 2).

Overall, it can be concluded that the release of SA from liposome happens very quickly but significantly slower compared to the control SA-PBS probe. As it can be seen, in vitro release of SA can be characterized by a biphasic profile. After 1 h, the percent of released SA from the liposomes was ~20%, while in the next 1 h measurements showed insignificantly higher release, ~25%. Values of SA release from the PBS (control sample) were about twice as high compared to SA liposomal dispersions (Fig. 2).
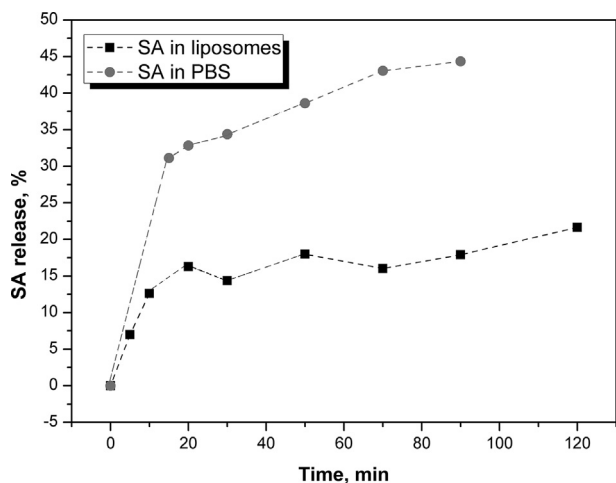
Fig. 2. Sulfanilamide release profiles from PBS and liposomes.

In order to obtain a better insight into the SA release kinetics, obtained experimental data were fitted to the appropriate mathematical models using *DDSolver* (zero order, first order, Higuchi, Korsmeyer-Peppas and Baker-Lonsdale), and the calculated parameters are shown in Table 1.

Based on the values of the determination coefficient (R^2), and AIC values, the model that best describes the SA release from liposomes is Korsmeyer-Peppas model (highest R^2 and lowest AIC). Due to the diffusion release exponent value, n = 0.236, it can be concluded that mechanism of drug release in Korsmeyer-Peppas model is based on the phenomenon of diffusion (Costa and Lobo, 2001).

3.3. UV irradiation of SA in PBS and liposomes

The second goal of this work was to examine stability of SA (in PBS and inside of liposomes) to the oxidative stress induced by continuously UV-A (350 nm), UV-B (300 nm) and UV-C (254 nm) irradiation, followed by absorption spectroscopy method. The

experiments were performed on three types of liposomes, SUV, LUV and MLV-SA liposomes made of 1,2-dimyristoyl-*sn*-glycero-3-phosphocholine lipid at different periods of time as shown in Fig. 3A–C. The SA stability was dependent on irradiation time and irradiation energy input of UV photons but also on the liposome size (Fig. 3).

From the sulfanilamide UV–Vis absorption spectra (not shown), it was evident a decrease in absorbance at 258 nm (SA absorption maximum), which indicate that SA alone, and in liposomes is photosensitive. The proportional appearance of new absorption
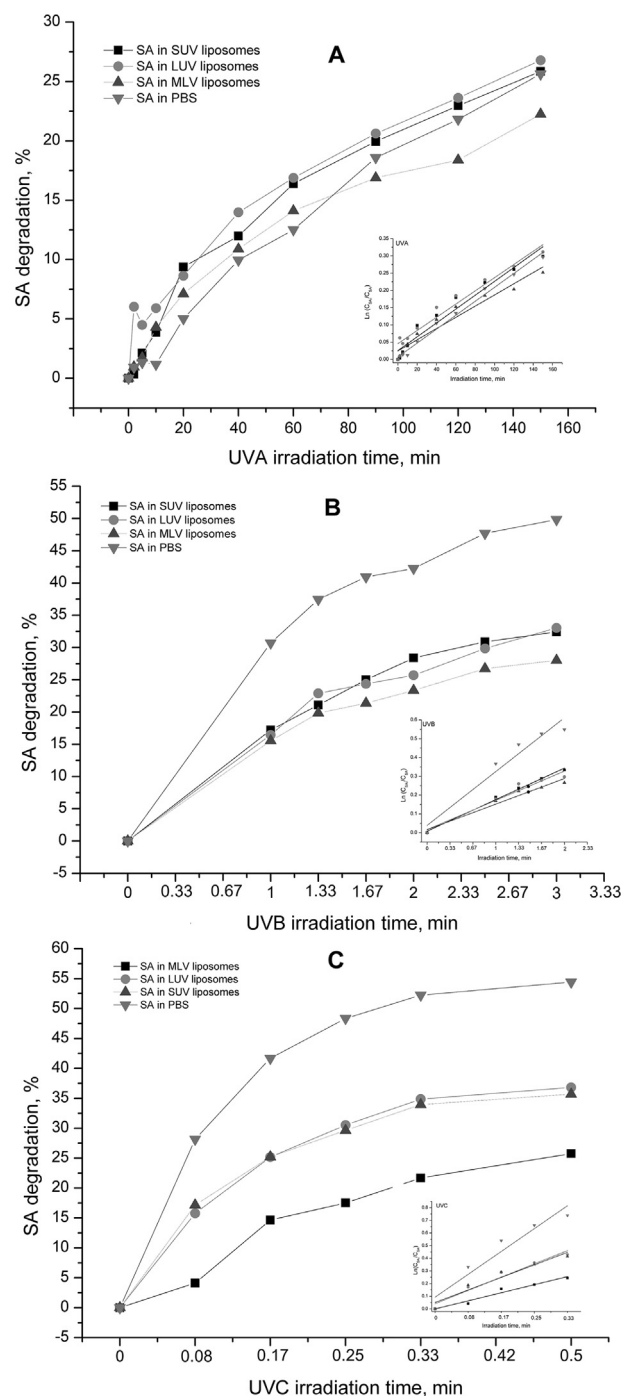
Table 1
In vitro SA release kinetics models.

Kinetic model	Parameter	SA in liposomes	SA in PBS
Zero order $f = k_0 \cdot t$	k_0 R^2 AIC	0.228 −0.2091 56.3222	0.651 0.0241 52.2794
First order $F = 100 \cdot [1 - e^{-k_1 \cdot t}]$	k_1 R^2 AIC	0.003 −0.0854 55.3514	0.010 0.3657 49.2628
Korsmeyer–Peppas $F = k_{KP} \cdot t^n$	k_{KP} n R^2 AIC	6.634 0.236 0.9254 33.2504	17.472 0.207 0.998 10.7935
Baker–Lonsdale $\frac{3}{2} \cdot \left[1 - \left(1 - \frac{F}{100}\right)^{2/3}\right] - \frac{F}{100} = k_{BL} \cdot t$	k_{BL} R^2 AIC	0 0.7102 43.4663	0.001 0.8672 38.32
Higuchi $F = k_H \cdot t^{1/2}$	k_H R^2 AIC	2.216 0.6833 44.2654	5.489 0.8123 40.739

R^2, coefficient of determination; AIC, Akaike Information Criterion; F is the fraction of drug released at time t; k_0 is the zero-order release constant; k_1 is the first-order release constant; k_{KP} is the release constant incorporating structural and geometric characteristics of the drug-dosage form; n is diffusion release exponent; k_{BL} is the combined constant in Baker-Lonsdale model; k_H is the Higuchi release constant (Costa and Lobo, 2001; Zhang et al., 2010; Đorđević et al., 2016).

Fig. 3. SA degradation (%) in SUV/LUV/MLV liposomes and in PBS induced by UV-A (A), UV-B (B) and UV-C (C) irradiation as a function of UV irradiation time. SA concentration in liposomes and in PBS was 1×10^{-5} M. In the Figures inserts are represented corresponding $\ln C_{SA0}/C_{SA} = f(t_{irr.})$ graphs.

maxima in UV–Vis spectra was noticed in the wavelength ranges of 300–350 and 550–600 nm in the case of all investigated samples. The intensity of these maxima is increased with increasing irradiation time which indicates the formation of degradation products that will be detected and characterized using the UHPLC/MS analysis in continuation. The results shown in Fig. 3 indicated an instability of SA to UV irradiation in the order to energy input strength by order, UV-A < UV-B < UV-C. SA degradation seems to be lowest in the case of MLV liposomes. The SA degradation in SUV and LUV liposomes was imperceptibly different which indicate that liposome size change from 100 to 400 nm had no influence to the SA distribution in liposomes. Also, instability to UV-A, B and C irradiation was higher in PBS (degradation % – 25.629, 49.830 and 54.522) compared to the liposomes (degradation, % – MLV: 22.250, 28.010 and 25.750; LUV: 26.770, 33.058 and 36.820; SUV: 25.841, 32.881 and 35.678), highlighting an increase in SA stability when it was incorporated into lipid vesicles.

Kinetics of SA degradation in PBS and liposomes (SUV, LUV and MLV) was investigated and respectively shown in Fig. 3A–C insets. The corresponding kinetic logarithmic plots are presented as a result of increasing time of irradiation for the SA in PBS as well as in liposomes of different size for all three UV-ranges, $\ln C_{SA0}/C_{SA} = f(t_{irr.})$. The rate constants, k, are calculated from the slopes (Eq. (1)) and presented in Table 2:

$$y = kx + n \qquad (1)$$

where:

– y is $\ln C_{SA0}/C_{SA}$,
– C_{SA0} is initial SA concentration,
– C_{SA} is SA concentration after certain irradiation time ($t_{irr.}$),
– x is the UV-irradiation time in minutes and
– k is the rate constant for the SA degradation (min^{-1}), shown in Table 2.

The UV-induced SA degradation in PBS and liposome vesicles fits the first-order kinetic that is common model for photochemical reactions (Veljkovic, 1969). The first order reactions include a number of processes of internal redeployment or substances decomposition present in the reaction mixture. In majority of first order reactions other components from the reaction mixture such as inert solvent molecules or other substances, also participate in the reaction. If the changes in these other molecules are small by scope and by their nature, they are not relevant so they can be ignored. If so, it can be assumed that degradation reaction speed in this case is subordinate mostly of SA. The plots show linear fits, with R^2 values of 0.93–0.99. The presented data (Table 2) suggest that the SA degradation rate *in vitro* depends on the UV irradiation range *i.e.*, the energy of the photons. It would be expected that SA in liposomes should be much more stable against UV radiation. However, based on data presented in Table 2, we can conclude that liposomes have stability role against SA-UV degradation (decreases of the k rates), except in the case of SA-SUV liposomes exposed to UVA irradiation where k values are similar to those reported in SA-PBS. The values of the calculated SA degradation rate constants, k, are in agreement with the somewhat different conditions of continuous UV-irradiation (such as energy flux and distance from the lamps). The lowest degradation rate constant is obtained in the case of SA in MLV liposomes for all three UV-ranges: UV-A, UV-B and UV-C.

3.4. Identification of UV irradiation SA degradation products by UHPLC-MS/MS analysis

In order to identify SA degradation products and SA degradation pathway after UV-irradiation UHPLC-MS/MS method was applied. The experiment was designed in a manner that standard solution of SA was firstly subjected to UHPLC-MS/MS analysis before sample irradiation. Obtained chromatograms of SA before and after UV-irradiations are shown in Fig. 4. The respondent parameters of identified compounds are presented in Table 3. As it can be seen from Fig. 4A, in SA standard solution presence of only one intensive peak at retention time 1.01 min was recorded. After MS fragmentation of its molecular peak at m/z 173.61, four new fragment ions at m/z 155.97, 125.03, 108.02 and 93.06 were obtained (Table 3). The resulting SA fragment ions are in agreement with previously published results by Liu et al. (2011). Absorption spectra obtained from UV–Vis UHPLC detector additionally confirms that peak at 1.01 min originate from SA (Khankhasaeva et al., 2015). The results after UV-A, B and C irradiation of SA are presented in Fig. 4B–D, respectively. The presence of three new peaks in chromatograms,
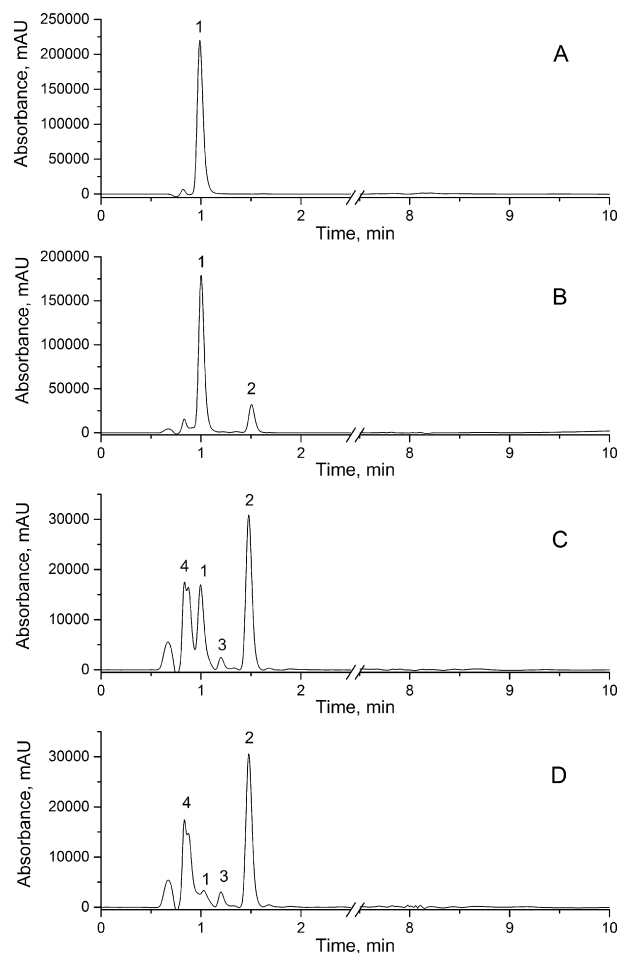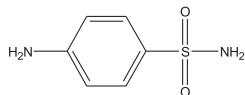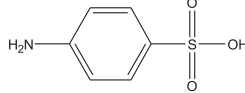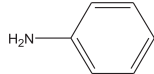
Table 2
Rate constants, k (min^{-1}), calculated from the slopes of the corresponding kinetic logarithmic plots $\ln C_{SA0}/C_{SA} = f(t_{irr.})$.

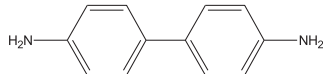| Medium	UV-irradiation wavelength, nm		
	UV-A (350 nm)	UV-B (300 nm)	UV-C (254 nm)
	k (min^{-1})		
SUV (100 nm)	0.00201	0.00280	0.01985
LUV (400 nm)	0.00191	0.00259	0.02099
MLV (1000 nm)	0.00162	0.00227	0.01278
PBS	0.00202	0.00477	0.03616

Fig. 4. UHPLC chromatograms of sulfanilamide (A) and sulfanilamide after UV-A (B), UV-B (C) and UV-C irradiation (D). SA concentration was 1×10^{-5} M.

Table 3
Characteristic parameters of identified compounds after UV irradiation of SA.

Peak No	t_R, min	Molar mass	[M + H]+	MS/MS	λ_{max}, nm	Compound	Molecular structure
1	1.01	172.03	173.61	155.97 125.03 108.02 93.06	262	Sulfanilamide	
2	1.51	173.01	174.03	156.01 108.02 93.03	249	Sulfanilic acid	
3	1.19	93.05	94.05	81.03 77.03 51.02	232 284	Aniline	
4	0.82	184.01	185.01	180.68 166.94 142.52 102.21	286	Benzidine	

labeled as 2, 3, and 4 can be observed. MS fragmentation data and PDA spectrum data of new detected products are presented in Table 3. After UV-A irradiation (Fig. 4B) presence of sulfanilic acid was detected. In UV-B and UV-C irradiation chromatograms, beside sulfanilic acid two new degradation products (peaks 3 and 4) were recorded. Peaks 3 and 4 are identified as aniline and benzidine, respectively.

Based on the peak area, it can be concluded that amount of sulfanilic acid is the highest compared to the other incurred degradation products. Also, it can be observed that degradation of SA is the highest after UV-C irradiation. The same degradation products identified after three different types of UV irradiation (UV-A, UV-B and UV-C) point to the same SA degradation mechanism. SA is sensitive to photo-oxidation due to the presence of aniline in its structure (Albini and Fasani, 2004). UV irradiation may lead to production of free radicals in organic compounds, especially those containing C=C bonds. In SA these bonds appear in great numbers. Once created, free radicals can initiate chain reactions, which, in some cases, may be linked particularly to the presence of C=C bonds. In accordance with literature data (Albini and Fasani, 2004), after UV-irradiation the potential photodegradation products of SA are azo- and nitro- derivatives. If we take into consideration degradation products that are identified in investigations of Fenton type catalysis of SA (El-Ghenymy et al., 2014; Khankhasaeva et al., 2015; Feng et al., 2016), degradation SA products identified in this work were identical. Since main obtained free radicals in Fenton reactions are ·OH radicals, we can assume that obtained SA degradation products after applied UV stress can be result of ·OH action (Wang et al., 2011). The formation of sulfanilic acid and aniline obvious is result of NH_2 group loss. In the case of sulfanilic acid formation, the NH_2 is replaced with OH group. In turn, formation process of benzidine or 1,1′-biphenyl-4, 4′-diamine, can be explained by recombination that occurs between radicals obtained in reaction mixture after UV irradiation. Once formed ·$C_6H_4NH_2$ are capable to interact with another ·C_6H_4-NH_2 free contributing to the benzidine generation.

4. Conclusion

Investigation of SA stability under influence of UV-A, UV-B and UV-C irradiation in PBS solution and in liposomes pointed to the liposomes protective role. The results showed SA instability to UV irradiation in order to the energy input strength: UV-A < UV-B < UV-C. Liposomes size also influenced the SA stability that was higher in MLVs compared to the SUVs and LUVs. *In vitro* drug release study demonstrated that liposomes with incorporated SA

contribute to the delayed SA distribution release that can be described by Korsmeyer–Peppas model. SA instability to the UV irradiation is reflected in sulfanilic acid, aniline and benzidine degradation products formation. SA degradation in PBS and liposome vesicles fits the first-order kinetic model. The degradation rate constants are dependent not only to involved UV photons energy input but also the SA microenvironment. The results obtained in this work could serve for further investigations of SA activity in potential active formulations.

References

Albini, A., Fasani, E., 2004. Rationalizing the photochemistry of drugs. In: Tønnesen, H.H. (Ed.), Photostability of Drugs and Drug Formulations. CRC Press, Boca Raton, pp. 67–111.

Baran, W., Sochacka, J., Wardas, W., 2006. Toxicity and biodegradability of sulfonamides and products of their photocatalytic degradation in aqueous solutions. Chemosphere 65 (8), 1295–1299.

Boreen, A.L., Arnold, W.A., McNeill, K., 2004. Photochemical fate of sulfa drugs in the aquatic environment: sulfa drugs containing five-membered heterocyclic groups. Environ. Sci. Technol. 38 (14), 3933–3940.

Brown, C.K., Friedel, H.D., Barker, A.R., Buhse, L.F., Keitel, S., Cecil, T.L., Kraemer, J., Morris, M., Reppas, C., Stickelmeyer, M., Shah, V., Yomota, C., 2011. FIP/AAPS joint workshop report: dissolution/in vitro release testing of novel/special dosage forms. Indian. J. Pharm. Sci. 73 (3), 338–353.

Burgess, D.J., Hussain, A.S., Ingallinera, T.S., Chen, M.L., 2002. Assuring quality and performance of sustained and controlled release parenterals: workshop report. AAPS Pharm. Sci. 4 (2), 13–23.

Chidambaram, N., Burgess, D.J., 1999. A novel in vitro release method for submicron-sized dispersed systems. AAPS J. 1 (3), 32–40.

Costa, P., Lobo, J.M.S., 2001. Modeling and comparison of dissolution profiles. Eur. J. Pharm. Sci. 13 (2), 123–133.

Delgado, D.R., Romdhani, A., Martinez, F., 2011. Thermodynamics of sulfanilamide solubility in propylene glycol+ water mixtures. Lat. Am. J. Pharm. 30 (10), 2024–2030.

Đorđević, S., Isailović, T., Cekić, N., Vuleta, G., Savić, S., 2016. Diazepam-loaded parenteral nanoemulsions: physicochemical characterization and in vitro release study. Arh. Farm. 66 (1), 24–41.

El-Ghenymy, A., Rodríguez, R.M., Brillas, E., Oturan, N., Oturan, M.A., 2014. Electro-Fenton degradation of the antibiotic sulfanilamide with Pt/carbon-felt and BDD/carbon-felt cells. Kinetics, reaction intermediates, and toxicity assessment. Environ. Sci Pollut. R 21 (14), 8368–8378.

Feng, Y., Liao, C., Shih, K., 2016. Copper-promoted circumneutral activation of H_2O_2 by magnetic $CuFe_2O_4$ spinel nanoparticles: mechanism, stoichiometric efficiency, and pathway of degrading sulfanilamide. Chemosphere 154, 573–582.

Gray, H.B., Simon, J.D., Trogler, W.C., 1995. Braving the Elements. University Science Books.

Henry, R.J., 1943. The mode of action of sulfonamides. Bacteriol. Rev. 7 (4), 175.

Khankhasaeva, S.T., Dambueva, D.V., Dashinamzhilova, E.T., Gil, A., Vicente, M.A., Timofeeva, M.N., 2015. Fenton degradation of sulfanilamide in the presence of Al, Fe-pillared clay: catalytic behavior and identification of the intermediates. J. Hazard. Mater. 293, 21–29.

Lam, M.W., Mabury, S.A., 2005. Photodegradation of the pharmaceuticals atorvastatin, carbamazepine, levofloxacin, and sulfamethoxazole in natural waters. Aquat. Sci. 67 (2), 177–188.

Liu, R., He, P., Li, Z., Li, R., 2011. Simultaneous determination of 16 sulfonamides in animal feeds by UHPLC-MS-MS. J. Chromatogr. Sci. 49 (8), 640–646.

Milenkovic, S.M., Bărbînţă-Pătraşcu, M.E., Baranga, G., Markovic, D.Z., Tugulea, L., 2013. Comparative spectroscopic studies on liposomes containing chlorophyll a and chlorophyllide a. Gen. Physiol. Biophys. 32 (4), 559–567.

Patrascu, M.E.B., Tugulea, L., Lacatusu, I., Meghea, A., 2010. Spectral characterization of model systems containing lipids and chlorophyll. Mol. Cryst. Liq. Cryst. 522 (1), 148–448.

Periša, M., Babić, S., Škorić, I., Frömel, T., Knepper, T.P., 2013. Photodegradation of sulfonamides and their N4-acetylated metabolites in water by simulated sunlight irradiation: kinetics and identification of photoproducts. Environ. Sci. Pollut. R 20 (12), 8934–8946.

Petrović, S.M., Tugulea, L., Marković, D.Z., Barbanta-Patrascu, M., 2014. Chlorophyll a and chlorophyllide a inside liposomes made of saturated and unsaturated lipids: a possible impact of the lipids microenvironment. APTEFF 45, 215–227.

Silverstein, R.M., Webster, F.X., Kiemle, D.J., Bryce, D.L., 2014. Spectrometric Identification of Organic Compounds. Wiley, New York.

Sukul, P., Spiteller, M., 2006. Sulfonamides in the environment as veterinary drugs. Rev. Environ. Contam. Toxicol. 187, 67–101.

Shen, J., Burgess, D.J., 2012. Accelerated in-vitro release testing methods for extended-release parenteral dosage forms. J. Pharm. Pharmacol. 64 (7), 986–996.

Tačić, A., Savić, I., Nikolić, V., Savić, I., Ilić-Stojanović, S., Ilić, D., Petrović, S., Popsavin, M., Kapor, A., 2014. Inclusion complexes of sulfanilamide with β-cyclodextrin and 2-hydroxypropyl-β-cyclodextrin. J. Incl. Phenom. Macro. 80 (1–2), 113–124.

Trovó, A.G., Nogueira, R.F., Agüera, A., Sirtori, C., Fernández-Alba, A.R., 2009. Photodegradation of sulfamethoxazole in various aqueous media: persistence, toxicity and photoproducts assessment. Chemosphere 77 (10), 1292–1298.

Varagić, V.M., Milošević, M.P., 2009. Farmakologija. Elitmedica, Beograd.

Veljkovic, R.S., 1969. Hemijska kinetika. Univerzitet u Beogradu, Gradjevinska knjiga-Beograd.

Wang, P., Zhou, T., Wang, R., Lim, T.T., 2011. Carbon-sensitized and nitrogen-doped TiO2 for photocatalytic degradation of sulfanilamide under visible-light irradiation. Water Res. 45 (16), 5015–5026.

Wittung, P., Kajanus, J., Kubista, M., Malmström, B.G., 1994. Absorption flattening in the optical spectra of liposome-entrapped substances. FEBS Lett. 352 (1), 37–40.

Zessel, K., Mohring, S., Hamscher, G., Kietzmann, M., Stahl, J., 2014. Biocompatibility and antibacterial activity of photolytic products of sulfonamides. Chemosphere 100, 167–174.

Zhang, Y., Huo, M., Zhou, J., Zou, A., Li, W., Yao, C., Xie, S., 2010. DDSolver: an add-in program for modeling and comparison of drug dissolution profiles. AAPS J. 12 (3), 263–271.